



## Extension and statistical analysis of the GACP aerosol optical thickness record



Igor V. Geogdzhayev<sup>a,b,\*</sup>, Michael I. Mishchenko<sup>b</sup>, Jing Li<sup>a,b,c</sup>, William B. Rossow<sup>d</sup>, Li Liu<sup>a,b</sup>, Brian Cairns<sup>b</sup>

<sup>a</sup> Columbia University, 2880 Broadway, New York, NY 10025, USA

<sup>b</sup> NASA Goddard Institute for Space Studies, 2880 Broadway, New York, NY 10025, USA

<sup>c</sup> Scripps Institute of Oceanography, 8622 Kennel Way, La Jolla, CA 92037, USA

<sup>d</sup> Department of Electrical Engineering, The City College of New York, Steinman Hall, 140th Street & Convent Avenue, New York, NY 10031, USA

### ARTICLE INFO

#### Article history:

Received 10 December 2014

Received in revised form 18 May 2015

Accepted 22 May 2015

Available online 28 May 2015

#### Keywords:

Tropospheric aerosols

Aerosol remote sensing

Optical thickness

Global Aerosol Climatology Project

Long-term trends

Principal Component Analysis

### ABSTRACT

The primary product of the Global Aerosol Climatology Project (GACP) is a continuous record of the aerosol optical thickness (AOT) over the oceans. It is based on channel-1 and -2 radiance data from the Advanced Very High Resolution Radiometer (AVHRR) instruments flown on successive National Oceanic and Atmospheric Administration (NOAA) platforms. We extend the previous GACP dataset by four years through the end of 2009 using NOAA-17 and -18 AVHRR radiances recalibrated against MODerate resolution Imaging Spectroradiometer (MODIS) radiance data, thereby making the GACP record almost three decades long. The temporal overlap of over three years of the new NOAA-17 and the previous NOAA-16 record reveals an excellent agreement of the corresponding global monthly mean AOT values, thereby confirming the robustness of the vicarious radiance calibration used in the original GACP product. The temporal overlap of the NOAA-17 and -18 instruments is used to introduce a small additive adjustment to the channel-2 calibration of the latter resulting in a consistent record with increased data density. The Principal Component Analysis (PCA) of the newly extended GACP record shows that most of the volcanic AOT variability can be isolated into one mode responsible for ~12% of the total variance. This conclusion is confirmed by a combined PCA analysis of the GACP, MODIS, and Multi-angle Imaging SpectroRadiometer (MISR) AOTs during the volcano-free period from February 2000 to December 2009. We show that the modes responsible for the tropospheric AOT variability in the three datasets agree well in terms of correlation and spatial patterns. A previously identified negative AOT trend which started in the late 1980s and continued into the early 2000s is confirmed. Its magnitude and duration indicate that it was caused by changes in tropospheric aerosols. The latest multi-satellite segment of the GACP record shows that this trend tapered off, with no noticeable AOT change after 2002. This result is consistent with the MODIS and MISR AOT records as well as with the recent gradual reversal from brightening to dimming revealed by surface flux measurements in many aerosol producing regions. Thus the robustness of the GACP record is confirmed, increasing our confidence in the validity of the negative trend. Although the nominal negative GACP AOT trend could partially be an artifact of increasing aerosol absorption, we argue that the time dependence of the GACP record, including the latest flat period, is more consistent with the actual decrease in the tropospheric AOT.

© 2015 Elsevier B.V. All rights reserved.

### 1. Introduction

Improving the ability of general circulation models to reproduce the past and forecast the future climate variability requires reliable knowledge of the global aerosol distribution in the terrestrial atmosphere. Tropospheric aerosols contribute significantly to climate change via direct and indirect radiative effects, but the magnitude of this contribution remains highly uncertain (Hansen et al., 2005; IPCC, 2007; Kiehl, 2007; Loeb and Su, 2010; Lohmann and Ferrachat, 2010; Penner et al., 2011).

Satellite datasets with their long-term record and near-global quasi-uniform coverage represent a unique source of information about atmospheric aerosols. One of the main objectives of the Global Aerosol Climatology Project (GACP; Mishchenko et al., 2002a) established in 1998 as part of the National Aeronautics and Space Administration (NASA) Radiation Sciences Program and the Global Energy and Water Cycle Experiment was to perform a retroactive analysis of the National Oceanic and Atmospheric Administration (NOAA) Advanced Very High Resolution Radiometer (AVHRR) radiance dataset in order to infer a multi-decadal pattern of the global distribution of aerosols and its seasonal and interannual variations. As such, the GACP record is based on data from an instrument that was not originally intended for aerosol retrievals and has a number of inherent limitations, e.g., the

\* Corresponding author at: Columbia University, 2880 Broadway, New York, NY 10025, USA. Tel.: +1 212 678 5511; fax: +1 212 678 5622.

E-mail address: [igor.v.geogdzhayev@nasa.gov](mailto:igor.v.geogdzhayev@nasa.gov) (I.V. Geogdzhayev).

absence of polarimetric and/or multiangular measurements, the lack of on-board calibration, and the availability of only two closely spaced and relatively broad visible/near-infrared channels. Thus, the AVHRR lacks many features of the next-generation instruments such as the MODerate resolution Imaging Spectroradiometer (MODIS; King et al., 2003; Remer et al., 2008; Levy, 2009), the Multi-angle Imaging SpectroRadiometer (MISR; Diner et al., 1998; Kahn et al., 2009; Martonchik et al., 2009), and the POLarization and Directionality of the Earth's Reflectance instrument (POLDER; Tanré et al., 2011).

Nevertheless, the use of the GACP aerosol record has proved to be essential and has yielded important insights into aerosol changes owing to two key factors: (i) the AVHRR instruments have been continuously operational since the early 1980s onboard successive NOAA satellites, thereby yielding one of the longest global aerosol datasets available; and (ii) the period covered encompasses two major volcanic eruptions (El Chichon in March 1982 and Mt Pinatubo in June 1991). The longevity of the GACP record has made it possible to analyze long-term trends in the global aerosol distribution. In particular, Mishchenko et al. (2007a) reported a likely decreasing trend in the global optical thickness of tropospheric aerosols over oceans between the late 1980s and early 2000s consistent with the contemporaneous switch from global dimming to global brightening at locations where surface solar flux has been measured (Wild, 2012). Mishchenko and Geogdzhayev (2007) further analyzed regional trends in both aerosol optical thickness (AOT) and size and identified decreased tropospheric aerosol loadings over much of Europe and a significant part of the Atlantic Ocean as well as increasing trends over long stretches of African and Asian coasts qualitatively consistent with the results of extensive ground-based observations and recent emission-inventory assessments (similar results were reported by Zhao et al., 2008). In agreement with the regional GACP results, Yoon et al. (2014) found a statistically significant AOT decrease over Europe and an increase over China between 2003 and 2008 based on data from multiple instruments. Li et al. (2014a) applied the Principal Component Analysis (PCA) to the GACP record in order to better separate the effects of volcanic and tropospheric aerosols. Their analysis confirmed a decrease in the global AOT between the late 1980s and early 2000s.

It is important to keep in mind however that by necessity, the GACP retrieval algorithm is based on the assumption of a temporally and spatially fixed aerosol refractive index value. Therefore, a trend in the retrieved AOT may not directly imply a trend in the aerosol amount, as changes in the aerosol optical properties may bias AOT retrievals. Mishchenko et al. (2012) analyzed the retrieval implications of allowing the imaginary part of the aerosol refractive index  $Im(m)$  to change over the duration of the GACP record. Their sensitivity study showed that increasing  $Im(m)$  from 0.003 during the 4-year pre-Pinatubo period up to 0.007 during the 4-year segment of GACP data ending in December of 2005 could eliminate the previously identified long-term decreasing AOT trend.

It is thus clear that, given the inherent limitations of the AVHRR instruments, one should make sure that conclusions about global aerosol changes based on the GACP record alone are consistent with other evidence. These consistency checks may come from validation using in-situ data (Liu et al., 2004; Geogdzhayev et al., 2005; Smirnov et al., 2006) or from statistical analyses and external datasets such as those mentioned above.

The objective of this paper is twofold. First, we aim to further improve and analyze the GACP record by adding NOAA-17 and -18 AVHRR observations. Specifically, we extend the previous GACP record by four years through the end of 2009, thereby making it 26.5 years long. Also, we exploit the fact that the NOAA-17 AVHRR radiances have been recalibrated against the MODIS radiances to further examine the robustness of the radiance calibration approach used in the original GACP record. We use the temporal overlap of the NOAA-17 with NOAA-16 and -18 data to produce a consistent record with increased data density, expecting that good agreement between the data records

from multiple satellites would confirm the robustness of the cumulative data record and further support previous conclusions about long-term aerosol changes.

Second, we perform a statistical analysis of the cumulative GACP record and compare it with more advanced recent satellite datasets. We find that (i) the statistical modes and the spatial patterns of the GACP data agree very well with MODIS and MISR data for the volcano-free period between February 2000 and December 2009; (ii) the magnitude and the duration of the negative AOT trend between the late 1980s and early 2000s exclude the post-Pinatubo stratospheric aerosols as the likely cause of the trend; and (iii) the observed absence of trends in the global GACP AOT after 2002 is consistent with the contemporaneous MODIS and MISR results and data on global dimming/brightening. These lines of evidence strengthen our confidence in the previously identified negative trend in the global tropospheric AOT over the oceans.

## 2. Data

The nominal GACP product is documented in Mishchenko et al. (1999), Geogdzhayev et al. (2002), and Mishchenko and Geogdzhayev (2007) and can be obtained from <http://gacp.giss.nasa.gov>. It is based on analyzing AVHRR channel-1 and -2 radiance data over the oceans provided by the International Satellite Cloud Climatology Project (ISCCP) DX dataset (Rossow and Schiffer, 1999). The DX product includes a gridded and calibrated version of the AVHRR Global Area Coverage data sub-sampled at 30 km intervals. The previous GACP record was based on data from the following sun-synchronous polar-orbiting platforms: NOAA-7 (August 1981–January 1985), NOAA-9 (February 1985–October 1988), NOAA-11 (November 1988–September 1994), NOAA-14 (February 1995–June 2001), and NOAA-16 (October 2001–December 2005). Auxiliary information about the column ozone and water amounts was taken from the ISCCP version of the Television Infrared Observational Satellite Operational Vertical Sounder (TOVS) data.

During the period covered by the previous GACP record, the AVHRR instruments were flown on two sets of NOAA satellites: the afternoon platforms (NOAA-7, -9, -11, -14, -16), with the local equator crossing time at launch around 2:00 pm, and the morning platforms (NOAA-10, -12, -15), with the local equator crossing time before 8:00 am. Over the course of a satellite's life its orbit typically drifts further into the evening or morning hours for the afternoon and morning satellites, respectively. The previous GACP record was based solely on the data from the afternoon AVHRR instruments because radiances measured from the morning satellites are typically too low to yield reliable aerosol retrievals. However, the NOAA-17 platform launched in 2002 had the equator crossing time near 10:00 am, i.e., 2 h later than the previous morning satellites. This crossing time remained stable through the end of 2009. The resulting improvement in illumination conditions allowed us to use the NOAA-17 AVHRR data in addition to the afternoon NOAA-18 data to extend the GACP record. This also created a significant period of overlap between the afternoon NOAA-16 and -18 data on one hand and the morning NOAA-17 data on the other, increasing the density of the GACP dataset.

Note that consistent with the nominal usage accepted in the remote sensing literature, in this study we refer to a "global" GACP AOT. One should bear in mind however that in general, passive remote sensing instruments in sun-synchronous orbits do not provide reliable retrievals for large solar zenith angles. As a consequence, their useful coverage represents a wide belt of geographic latitudes which seasonally shifts to the north during the boreal summer and to the south during the boreal winter. The global distribution of clouds also affects the coverage of satellite-based aerosol retrievals. A quantitative analysis of the effects of coverage on global AOT estimates was performed by Geogdzhayev et al. (2014) using MODIS L2 aerosol data and daily global aerosol fields generated by several global circulation models.

In addition, in this study we use Level 3 monthly mean MODIS-Terra and MISR aerosol data to assess the resulting cumulative GACP product for the period from 2000 to 2009. We use the MODIS collection 5.1 AOT data available from the NASA Goddard Space Flight Center's Atmosphere Archive and Distribution System (<http://ladsweb.nascom.nasa.gov>). The MISR AOT product was obtained through the NASA Langley Research Center's Atmospheric Sciences Data Center (<http://eosweb.larc.nasa.gov>). The spatial resolution of the MODIS Level-3 data is  $1^\circ \times 1^\circ$ , while the resolution of the MISR Level-3 data was coarsened from the original  $0.5^\circ \times 0.5^\circ$  to  $1^\circ \times 1^\circ$ .

### 3. GACP retrieval algorithm and data analysis methodology

The GACP retrieval algorithm yields the column-integrated AOT and column-averaged Ångström exponent (AE) for each cloud-free ISCCP DX pixel. This is done by minimizing the difference between the AVHRR radiances measured at 0.65 and 0.85  $\mu\text{m}$  for the instantaneous illumination and observation angles determined by the satellite orbit and the radiances simulated theoretically for a realistic atmosphere-ocean model. The AE is defined according to

$$A = - \left. \frac{d[\ln C_{\text{ext}}(\lambda)]}{d(\ln \lambda)} \right|_{\lambda=\lambda_1}, \quad (1)$$

where  $\lambda_1 = 0.65 \mu\text{m}$  is the nominal wavelength of AVHRR channel 1 and  $C_{\text{ext}}$  is the ensemble-averaged extinction cross section per particle. The GACP retrievals are limited to areas over large water bodies such as oceans, seas, and lakes, in which case the surface reflectance is often low and can be adequately parameterized in the radiative-transfer model.

Aerosol properties are inferred from only two measurements per pixel, viz., AVHRR channel-1 and -2 radiances. This makes the retrieval a highly underdetermined procedure in which one must fix all model parameters other than AOT and AE a priori. In particular, we assume that the aerosol particles are homogeneous spheres and compute their scattering and absorption properties using the standard Lorenz-Mie theory (Mishchenko et al., 2002b). The aerosol complex refractive index is taken to be wavelength-independent and fixed at  $1.5 + i0.003$ , while the aerosol-particle size distribution is given by the following modified power-law function (Mishchenko et al., 1999):

$$n(r) = \begin{cases} C, & r \leq r_1 \\ C(r/r_1)^{-\alpha}, & r_1 < r \leq r_2 \\ 0, & r > r_2 \end{cases} \quad (2)$$

where  $r_1 = 0.1 \mu\text{m}$ ,  $r_2 = 10 \mu\text{m}$ , and  $\alpha \in [2.5, 5]$ . The normalization constant  $C$  is always chosen such that

$$\int_0^\infty dr n(r) = 1, \quad (3)$$

while the above range of  $\alpha$ -values translates into a representative AE range.

Theoretical channel-1 and -2 radiances are then simulated using a radiative transfer code based on the scalar version of the adding/doubling method (Hansen and Travis, 1974). The numerical procedure incorporates the rough ocean surface reflection (via the modified Kirchhoff approximation; Mishchenko and Travis, 1997), the water vapor, oxygen, and  $\text{CO}_2$  absorption (via the k-distribution technique; Lacis and Oinas, 1991), and gaseous (Rayleigh) scattering. The upwelling radiances from the ocean body and foam scattering are modeled by adding a small Lambertian component to the ocean-surface bidirectional reflection function. The vertical distributions of ozone and water vapor are based on standard atmospheric profiles (McClatchey et al., 1972). For simplicity, the vertical profile of aerosols is taken to be the

same as the normalized profile of water vapor. The radiative transfer code is used to compute a look-up table (LUT) in which multidimensional arrays of simulated channel-1 and -2 reflectance values for all viewing geometries and aerosol and atmospheric parameters are stored. The LUT is then used to retrieve the AOT and AE by fitting cloud-screened AVHRR channel-1 and -2 radiance data. Each pixel is mapped onto a  $1^\circ \times 1^\circ$  global grid. The retrieved AOT and AE values for all pixels within one grid cell are averaged to produce a map for a specified period of time. A more detailed description of the retrieval process can be found in Mishchenko et al. (1999).

The sensitivity analysis by Mishchenko et al. (1999, Section 3.J) demonstrates that retrieving the AOT simultaneously with the AE improves the accuracy and stability of the AOT retrieval. This is because at scattering angles typical of aerosol observations from space, the aerosol phase function can vary strongly with aerosol size. As a consequence, a fixed AE value in the retrieval algorithm can result in large errors (exceeding 300%) in the retrieved AOT. On the other hand, the sensitivity of the AVHRR observations to the aerosol AE itself is limited due to the fact that the central wavelengths of channels 1 and 2 are closely spaced. Furthermore, aerosol retrievals are usually performed at the lowest radiance levels, where small absolute calibration errors can cause a significant imbalance between the two channels and thereby affect the retrieved AE values. Given the limited accuracy and stability of the AVHRR AE record, we have decided not to treat it as a primary GACP product, although AE values continue to be determined internally by the retrieval algorithm. In other words, ball-park knowledge of the AE helps improve substantially the accuracy of the AOT retrieval but does not allow one to identify statistically significant global and regional trends in aerosol size.

Cloud screening is another major issue in aerosol retrievals from space. It affects retrievals directly because even a small cloud contamination of a pixel, if unnoticed, can cause a large artificial increase in the retrieved AOT. Clouds also influence the global AOT record indirectly by reducing the statistical weight of the regions where clouds are frequent (Geogdzhayev et al., 2014; Yoon et al., 2014). The GACP uses the standard ISCCP cloud detection algorithm (Rossow and Garder, 1993a, 1993b) with an additional infrared (IR) threshold test using AVHRR channel 5 (11.7  $\mu\text{m}$ ) reflectances. Specifically, we retain only pixels that are warmer than composite clear-sky IR temperatures estimated by the standard ISCCP cloud detection scheme by 1 K or more. The reason why the additional IR test is needed is because the ISCCP algorithm was designed primarily as a conservative cloud detection algorithm (whereby most pixels for which the presence of a cloud is in doubt are declared cloud free), whereas aerosol retrievals require a conservative cloud screening algorithm (whereby pixels for which the presence of a cloud is in doubt are declared cloudy). Further details on GACP cloud screening can be found in Mishchenko et al. (1999).

Fig. 1 shows the relative frequency of cloud-screened ISCCP DX pixels as a function of latitude for July 2005 (upper panel) and December 2005 (lower panel). Light gray bars are for all pixels available before cloud screening but after other tests (e.g., sun-glint test) have been applied; dark gray bars are for pixels available after the standard ISCCP cloud test has been applied; and black bars are for pixels available after the ISCCP standard test and the additional IR-threshold screening have been applied. First, one can see that the latitudinal distribution of the pixels available before cloud screening varies with season, reflecting the orbital changes discussed in the preceding section. The distribution also reflects the relative abundance of the water-covered surface. In addition it is significantly influenced by the exclusion of pixels contaminated by sun glint. The number of glint-contaminated pixels is a function of the satellite orbit, latitude, and season (cf. Geogdzhayev et al., 2014). Second, the application of the standard ISCCP cloud test reduces the number of available pixels by two-thirds on average with some variation with latitude and season. Of the pixels that have passed the ISCCP test, over 80% are rejected based on the additional IR test so that on

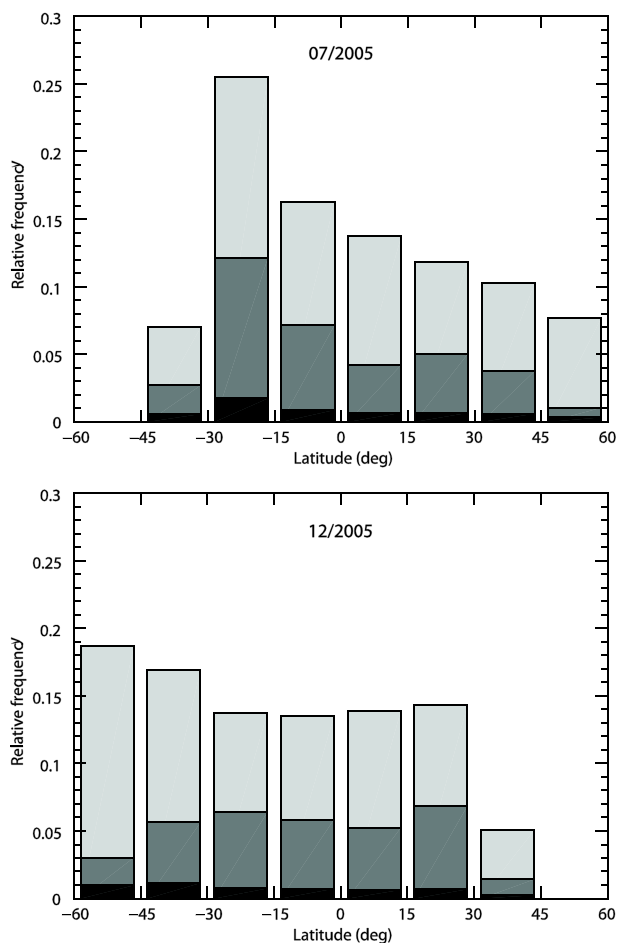


**Fig. 1.** Relative frequency of cloud-screened ISCCP DX pixels as a function of latitude for July 2005 (upper panel) and December 2005 (lower panel).

average, only about 5% of the pixels available before cloud screening are ultimately used for aerosol retrievals.

In Section 5 we use the Principal Component Analysis (PCA, a.k.a. Empirical Orthogonal Functions, or EOFs) to analyze AVHRR data and, in particular, to isolate the volcanic aerosol signal. The Combined Principal Component Analysis (CPCA) is used to assess the AVHRR tropospheric aerosol modes using Terra-MODIS and MISR data. Note that the PCA is widely applied to identify leading orthogonal modes of variability in multidimensional data by decomposing the data covariance matrix into a set of independent eigenvectors, with each eigenvector explaining a progressively smaller part of the total variance (Bjornsson and Venegas, 1997). The details of the application of PCA and CPCA are given in Appendix A.

Note that Levy et al. (2010) identified a bias in the MODIS Terra global AOT resulting in an overestimation by  $\sim 0.005$  before 2004 and an underestimation by a similar amount thereafter. The bias was found to be associated with uncertainties in the instrumental calibration. It mainly influences the trends of the Terra AOT time series, whereas the variability is much less affected. Previous studies comparing the spatial and temporal variabilities of data from Terra MODIS and several other satellite datasets had demonstrated that the variability of the Terra MODIS record agrees quite well with those of Aqua MODIS, MISR, and SeaWiFS (Li et al., 2013), as well as with that of AERONET (Li et al., 2014b, 2014c) (cf. Figs. 2–9 in Li et al., 2013 and Figs. 3 and 5 in Li et al., 2014c). In this study we use the MODIS Terra data (along with the MISR data) because of their longer temporal overlap with the GACP record compared to that of the MODIS Aqua data. The data are used to compare the variability and to interpret statistical modes. We

therefore believe that the bias identified by Levy et al. (2010) does not affect in any significant way the results of this study.

#### 4. Extension of the GACP record using NOAA-17 and -18 AVHRR data

As indicated in Section 2, we use the data from the NOAA-17 AVHRR to extend the GACP record by four years through the end of 2009, the last year for which the ISCCP DX data are currently available. We have already mentioned that the absence of an in-flight calibration capability is a significant problem potentially affecting the accuracy of AVHRR aerosol retrievals. Over the years a number of vicarious calibration methodologies have been proposed in order to account for the temporal degradation of the AVHRR instruments (e.g., Che and Price, 1992; Kaufman and Holben, 1993; Rao and Chen, 1995; Heidinger et al., 2010; Li et al., 2014d). As part of its overall data processing flow, the ISCCP procedure includes a consistent re-calibration of channel-1 reflectances from the AVHRR instruments flown on multiple NOAA platforms anchored on NASA ER-2 under-flights in the late 1980s (Brest et al., 1997). The original GACP product was based on these ISCCP-calibrated channel-1 radiances as well as on published NOAA-calibrated channel-2 radiances with some adjustments, as described in Geogdzhayev et al. (2002) and Mishchenko et al. (2003).

The two MODIS instruments flown on the NASA Terra and Aqua platforms since 2001 and 2003, respectively, are radiometrically more accurate and stable owing to the presence of an on-board calibrator. Heidinger et al. (2010) derived a set of reflectance calibration coefficients for all AVHRR instruments that are tied to the MODIS observations (when contemporaneous data are available). The calibration provided by Heidinger et al. (2010) is based on simultaneous nadir overpasses between AVHRR and MODIS instruments as well as on matching observations over stable targets such as the Libyan Desert and Greenland. In both cases the illumination and observational geometry of the instruments are taken into account, which suggests that diurnal cycles as observed by different satellites should not affect the calibration directly. Unlike the case with the ISCCP, the calibration coefficients are provided for both channel-1 and -2 radiances.

Comparisons of ISCCP channel-1 calibration coefficients with those published by Heidinger et al. (2010) showed that they agree within statistical uncertainties except for NOAA-15 and NOAA-17 (Rossow and Ferrier, 2015). Because one of the goals of this study is to extend the GACP record using NOAA-17 as well as NOAA-18 data and to examine their consistency with the previous NOAA-16 aerosol retrievals, we decided to use the calibration provided by Heidinger et al. for the NOAA-17 and -18 radiances. This was accomplished by directly applying the calibration coefficients to channel-2 AVHRR digital counts, while for channel 1 a set of monthly multiplicative factors was used to convert from ISCCP-calibrated reflectances. These factors were derived as part of the ISCCP calibration intercomparison and describe the relationship between the gains for the two calibration sets (Rossow and Ferrier, 2015). Given the good agreement between the ISCCP calibration and that derived by Heidinger et al. (2010), we found that no changes in the calibration of the previous GACP record (based on data from instruments up to and including NOAA-16) were required.

Fig. 2 shows the original GACP time series of the global monthly AOT over the oceans. It is seen that the AVHRR data record is strongly influenced by two volcanic eruptions, viz., the El Chichon eruption in March 1982 and the Mt Pinatubo eruption in June 1991. The NOAA-11 AVHRR failed at the end of 1994, i.e., before data from the NOAA-14 AVHRR became available in February of 1995, thereby causing a temporal gap in the data record. In addition, the NOAA-11 AVHRR data quality eventually deteriorated due to calibration problems and a strong orbital drift towards evening hours. Similarly, a strong drift of the NOAA-14 orbit is responsible for the gap in the data in 2001. A detailed analysis of the GACP aerosol data is available in Geogdzhayev et al. (2002, 2005), Mishchenko et al. (2007b), and Mishchenko and Geogdzhayev (2007).

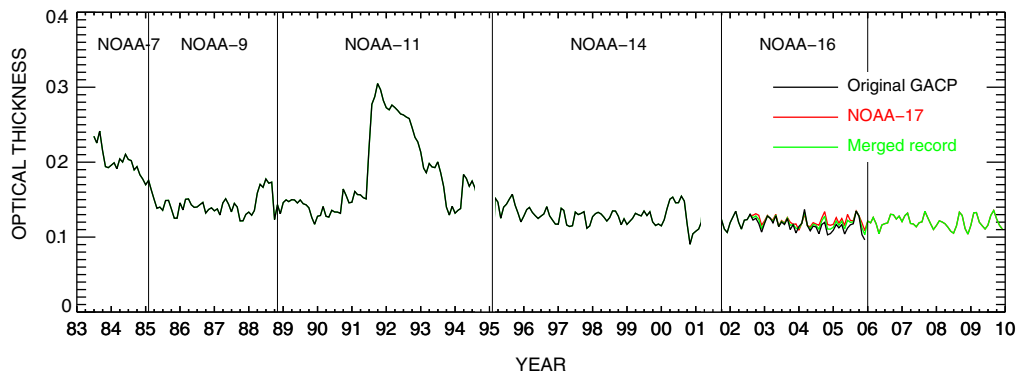


**Fig. 2.** Time series of the global AOT over the oceans. The black curve represents the previous GACP data, the red curve depicts the NOAA-17 data, and the green curve shows the merged dataset. The straight vertical lines mark the periods corresponding to AVHRR data from the different NOAA afternoon satellites.

Fig. 2 also shows the NOAA-17 retrievals covering the period between August 2002 and December 2009 and the merged data, thereby extending the original GACP record by four years. One can observe that the NOAA-17 global monthly AOT matches closely the nominal GACP record for the period of contemporaneous data (August 2002 through December 2005), the standard deviation between the two sets being just 0.0057. The two sets of AOT retrievals also exhibit similar seasonal variations with a high correlation coefficient of 0.78. To limit the effect of different geographical coverages of morning and afternoon satellites, the same statistics were computed for the equatorial region between the 30°S and 30°N latitudes. For this case the standard deviation was also found to be small, at 0.0070. As expected, this value is somewhat higher than in the previous case due to the smaller sample. The correlation coefficient remained unchanged, at 0.78. To investigate how temporal averaging affects the statistical agreement of the two records, the standard deviation and correlation coefficients were also computed for ten-day periods. We found that the standard deviation remained low, at 0.0066 and 0.0080 for the global and the equatorial samples, respectively, while the corresponding correlation coefficients remained high, at 0.77 and 0.78. The good agreement between the previous NOAA-16 and the new NOAA-17 AOT retrievals during an extended period of time (over 3 years) increases our confidence in the correctness and stability of the calibration used to compile the original GACP record. This conclusion is essential for the trend analysis presented in the next section. The residual discrepancies between the two AOT data sets may be due to differences in the geographic coverage of the NOAA-16 and -17 AVHRRs, a diurnal cycle of the global AOT, and/or transient events such as biomass burning.

The NOAA-18 AVHRR data in the ISCCP DX product cover the period between January 2006 and December 2009, which implies no overlap with the data from the previous afternoon NOAA-16 AVHRR ending in December 2005. Here we show how the NOAA-18 data can be assimilated into the extended GACP dataset to improve the spatial coverage density after 2005. Consistent with our previous approach, we use the calibration provided by Heidinger et al. (2010) for both visible channels of the NOAA-18 AVHRR. Note that the NOAA-18 AVHRR calibration provided by Heidinger et al. is nearly the same (within 2%) as the one provided by the ISCCP (Rossow and Ferrier, 2015). In addition, it was discovered that for the NOAA-18 AVHRR data between January 2006 and May 2007 in the ISCCP DX dataset the prelaunch calibration coefficients were not correctly included in the ISCCP calibration process. This resulted in the channel-1 reflectances being 0.01 higher. This problem was rectified by subtracting 0.01 from channel-1 reflectances before applying the multiplicative conversion coefficients mentioned previously for the affected months. Our initial analysis has shown that global monthly mean AOT values derived from the NOAA-18 AVHRR reflectances exceed the mean AOT from both the contemporaneous NOAA-17 data and the preceding NOAA-16 based retrievals by approximately

0.02. At the same time, the monthly mean NOAA-18 AVHRR channel-2 reflectance has been found to be  $\sim 0.00157$  higher (on average) than its NOAA-17 counterpart during the 4-year period between January 2006 and December 2009. We have found that adjusting the NOAA-18 channel-2 reflectances by this amount results in a much improved agreement: the standard deviation between the two data sets is a mere 0.00575, while the correlation coefficient is 0.76. Limiting the geographical coverage to between the 30°S and 30°N latitudes results in a slight increase of the standard deviation, to 0.0083, and a decrease of the correlation coefficient, to 0.68. A good statistical agreement remains for the ten-day averaging periods: the standard deviation and the correlation coefficient are 0.0059 and 0.81, respectively, for the entire sample, while for the tropical region the corresponding values are 0.0092 and 0.71.

This is illustrated in Fig. 3, which shows the NOAA-17 AOT record in black, the NOAA-18 AOTs in red, and the cumulative result in green. Importantly, the additive calibration adjustment discussed above is comparable to the accuracy with which the AVHRR space count is known and therefore does not contradict the calibration coefficients we use. In addition, the statistical agreement (standard deviation and correlation) between the contemporaneous NOAA-18 and NOAA-17 results is very similar to that between the contemporaneous NOAA-16 and NOAA-17 retrievals. Thus the temporal overlap of the NOAA-17 observations with both the NOAA-16 and the NOAA-18 measurements provides the requisite continuity of the merged AOT data record in which the adjusted NOAA-18 data are consistent with the previous NOAA-16 and -17 records. It also results in an improved spatial sampling density after August 2002.

## 5. Statistical analysis of the GACP AOT time series

As discussed before, perhaps the main advantage of the GACP record is its length. It covers the period during which two major volcanic eruptions occurred and long-term changes in natural as well as anthropogenic aerosol sources unfolded, with potentially significant effects on climate. It is therefore important to perform a statistical analysis of the global and regional changes in the retrieved AOT, especially in comparison with more advanced satellite data.

Here we use the statistical method outlined in Appendix A to identify orthogonal modes explaining the long-term variability of the GACP AOT. Statistically identified modes should then be subjected to physical interpretation as the natural causes of observed variability may not be strictly orthogonal and may affect more than one mode. In this study we supplement the analysis of Li et al. (2014a) using the newly extended GACP dataset. Li et al. (2014a, 2014c) have shown that many aerosol source regions governed by different emission and transport mechanisms and meteorological conditions can be isolated into different orthogonal modes by the PCA. In particular, volcanic aerosols are

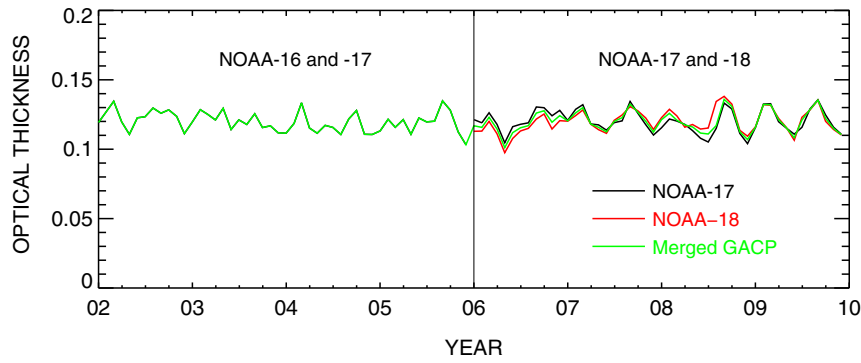


**Fig. 3.** Time series of the global AOT over the oceans showing the addition of the NOAA-18 data to the GACP record. Note the reduced vertical scale compared to Fig. 2. The black curve represents the NOAA-17 data, the red curve depicts the NOAA-18 results, and the green curve shows the merged dataset. The straight vertical line marks the transition from NOAA-16 to NOAA-18 afternoon satellites.

generally produced by sporadic eruptions and can reach the stratosphere, where their dependence on human activities and meteorological conditions is minimal. Therefore, the PCA may help separate the variability of volcanic aerosols from that of tropospheric aerosol species. This is important since passive satellite data typically yield column-integrated retrievals, thereby making it essential to distinguish stratospheric and tropospheric aerosol contributions.

Fig. 4 presents the first four orthogonal modes of the cumulative GACP AOD record. The left-hand column shows the spatial patterns of the modes, while the right-hand column shows the corresponding time series called principal components (PCs; see Li et al., 2013 for details).

The first PC shows a strong peak in 1991 resulting from the Mt Pinatubo eruption. The positive anomalies in the Mode 1 spatial pattern indicate a nearly uniform distribution over the tropical and subtropical areas which resembles the distribution of volcanic aerosols after the eruption. As can be seen from Fig. 4, most of the volcanic aerosol variability is isolated in a single mode (Mode 1) which is responsible for ~12% of the total variance. The time series of the first PC resembles closely the distribution of volcanic aerosols according to the Stratospheric Aerosol and Gas Experiment (SAGE) data (cf. Fig. 3 in Li et al., 2014a).

In order to confirm that Modes 2, 3, and 4 in Fig. 4 mostly represent the tropospheric aerosol variability, we applied a combined PCA, as

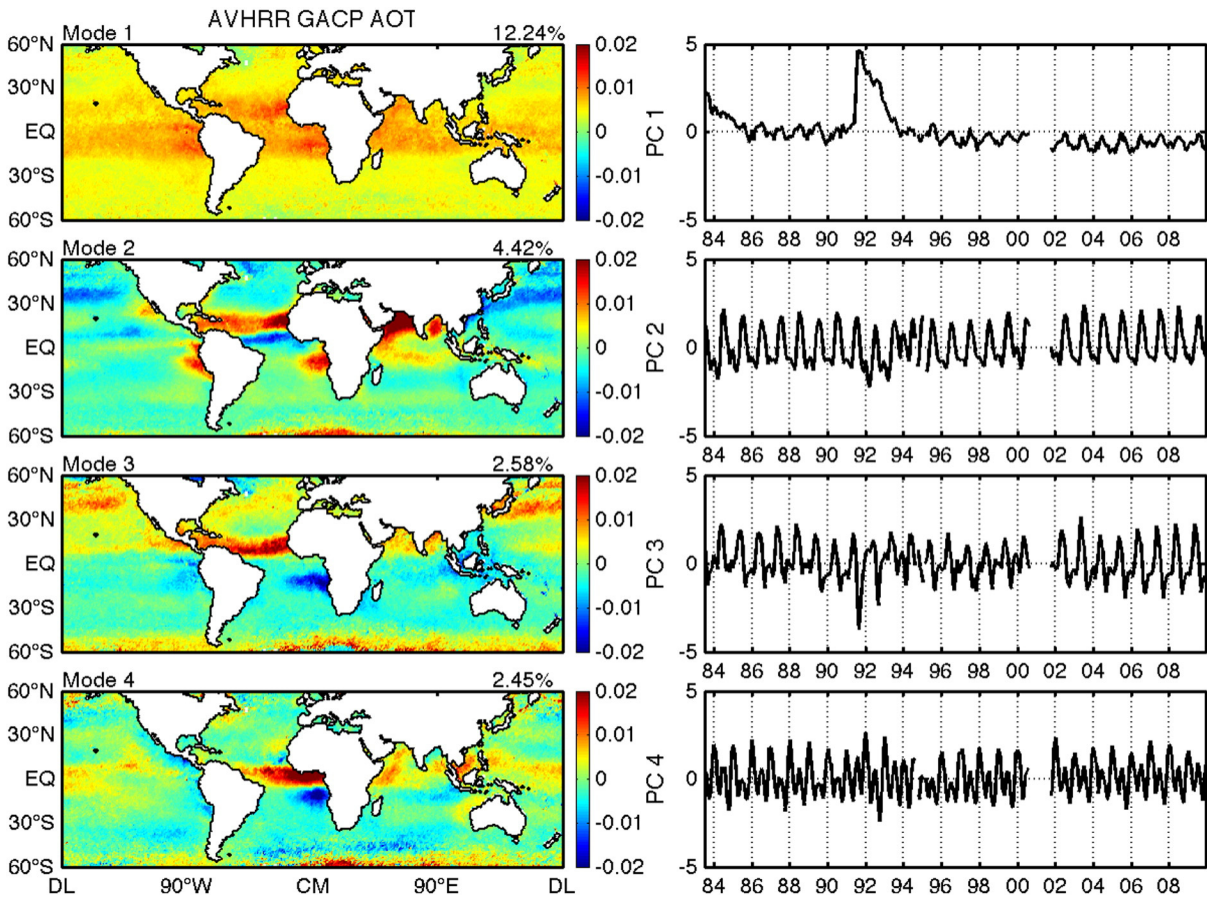


**Fig. 4.** PCA of the combined GACP AOT record from July 1983 to December 2009. The left-hand column shows the spatial patterns of the first four orthogonal modes, while the right-hand column depicts the corresponding PCs. The number above the top right-hand corner of each spatial map indicates the percentage of the total variance explained by the corresponding mode.

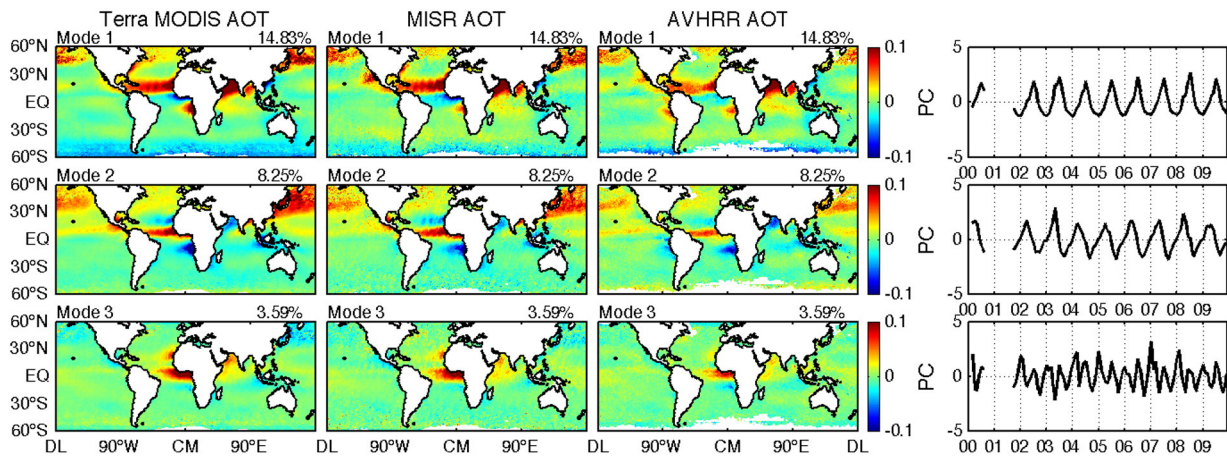


Fig. 5. Combined PCA of MODIS-Terra, MISR, and GACP AOT data for the volcano-free period from February 2000 to December 2009. The spatial patterns of the AVHRR data agree quite well with those for MODIS and MISR. These three modes are also in good agreement with Modes 2–4 in Fig. 4.

described by Li et al. (2014c), to the MODIS, MISR, and GACP AOT data corresponding to the volcano-free period between February 2000 and December 2009. The results for the first three modes are shown in Fig. 5. One can see that the spatial patterns of the GACP data agree very well with those of the MODIS and MISR data. The correlation between the spatial patterns of GACP and MODIS Modes 1, 2, and 3 is 0.77, 0.76, and 0.64, respectively, while that between the spatial patterns of GACP and MISR Modes 1, 2, and 3 is 0.75, 0.74 and 0.62, respectively. Moreover, Modes 1–3 in Fig. 5 strongly resemble Modes 2–4 in Fig. 4, with spatial correlations of 0.61, 0.60, and 0.66, respectively. PCs 2–4 in Fig. 4 and PCs 1–3 in Fig. 5 also capture, respectively, the same (boreal) summer–winter, spring–fall, and semi-annual seasonal cycles. This coherency indicates that Modes 2–4 in Fig. 4 indeed mostly represent the tropospheric aerosol variability. Nonetheless, there still exists some mode leakage for Mode 1 in Fig. 4, i.e., some tropospheric aerosols, including dust transported from North Africa and smoke transported for South America and South Africa, appear as positive signals and are mixed with the volcanic aerosols. This should also be the main reason of the observed weak seasonal variability of PC 1 in Fig. 4.

We note that sampling differences due to clouds and sun glint represent an important issue for aerosol retrievals from space and affect the observed statistical patterns (cf. Geogdzhayev et al., 2014). The uniformity of the coverage depends on the temporal and spatial scales. Daily satellite-based aerosol products are, in general, nonuniform at the scale of a hundred kilometers due to the clouds and sun glint (over

ocean). The MODIS or MISR coverage is significantly denser compared to that of GACP, making those datasets more suitable for the study of the sampling effects. However, at the one-degree scale of Fig. 5, the good agreement of the GACP monthly AOT PCA patterns with those of MODIS and MISR demonstrates that the sparser data density of the GACP product does not significantly affect its statistical characteristics. Since we cannot expect GACP to perform better than the newer aerosol missions given its inherent limitations, we find this result encouraging.

A downward trend in PC 1 is apparent from Fig. 4 between the pre-Pinatubo period and the early 2000s. We have already mentioned that a likely negative trend in the tropospheric AOT was identified during the same period by Mishchenko et al. (2007a). Fig. 6 shows the global monthly AOT anomaly time series for the actual GACP data (solid gray line) as well as for a “reduced” dataset obtained by subtracting Mode 1. The data between August 1994 and February 1995 and between June 2000 and June 2001 were excluded, as discussed in the preceding section. Also shown by the straight dashed lines are the corresponding linear trends for three distinct periods. During the quiescent period between the El-Chichon and Mt Pinatubo eruptions, both the actual and the reduced datasets are close to the long-term mean value, and no statistically significant trend is discernible. The second period is characterized by a linear negative trend. The actual data display a much stronger negative trend than the reduced data for this period:  $-0.0252/\text{decade}$  vs.  $-0.0067/\text{decade}$ , although both trends are statistically significant at the 95% level. While it was shown above that Mode 1 is mostly

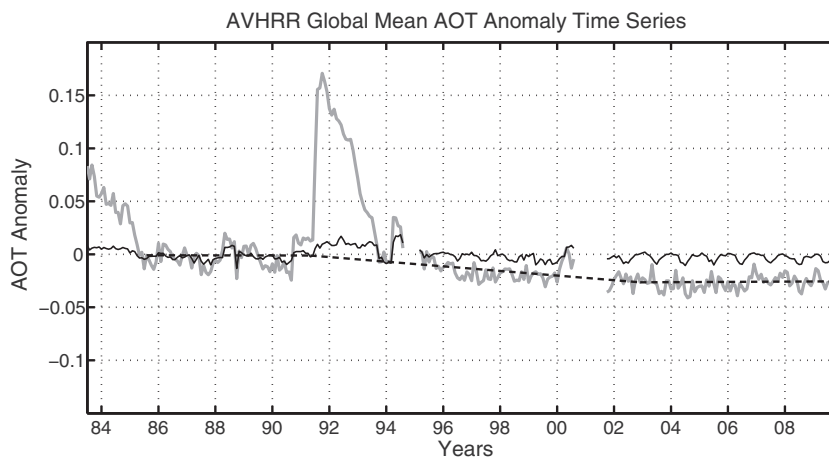


Fig. 6. Global time series and linear trends for the actual GACP data (solid gray curve) and data obtained by removing Mode 1 (solid black curve). Also depicted are the corresponding linear trends in the GACP AOT anomaly for the pre-Pinatubo period, the post-Pinatubo period, and for the most recent period starting in ~2002 (straight dashed lines).

responsible for the volcanic aerosol variability, the tropospheric–stratospheric aerosol separation between the modes is not perfect. This means that the purely statistical analysis may not be sufficient for the attribution of the observed trend. It should thus be interpreted on the basis of physical considerations.

The SAGE record indicates that the total stratospheric AOT remained stable at  $\sim 0.006$  after 1997 (cf. Fig. 3 in Li et al., 2014a). This suggests that the effects of the eruption on stratospheric aerosols wore off by that time. As is evident from Fig. 6, the negative AOT trend continued into the early 2000s. In addition, because of the small absolute value of the stratospheric AOT, any changes in it would be an order of magnitude smaller than the approximately  $-0.027$  AOT anomaly observed after 2002. These considerations as well as the supporting evidence discussed by Mishchenko and Geogdzhayev (2007) suggest that the observed AOT trend is caused by changes in tropospheric aerosols.

No statistically significant short-term tendencies are present in either the original or the reduced AOT anomaly data after  $\sim 2002$ . The absence of a trend in the average GACP AOT during this period is confirmed by the contemporaneous MODIS and MISR results (Mishchenko et al., 2009; Zhang and Reid, 2010; Chin et al., 2014) and is consistent with the accumulating evidence of a gradual recent transition from global brightening to global dimming (Wild, 2012, 2014; Zerefos et al., 2012).

As was pointed out by Mishchenko et al. (2012), the GACP data alone may not be sufficient to attribute the previously identified negative trend in the retrieved AOT to the global reduction in the aerosol amount or to changes in aerosol composition, e.g., to an increase in aerosol absorption. The possibility of an increased aerosol absorption that translated in an artificial reduction of the retrieved AOT cannot be completely excluded. However, to be a significant factor, the change in absorption (i) must be large (according to Mishchenko et al. (2012), excluding the possibility of an actual negative AOT trend requires an increase in the imaginary part of the refractive index from 0.003 to 0.007), and (ii) must be consistent with the temporal behavior of the combined GACP record. That is, the global aerosol absorption would have to increase between the late 1980s and early 2000s and then remain constant, thereby causing no further trend. This behavior is supported neither by analyses of the trends in the global black-carbon emissions and radiative forcings (e.g., Bond et al., 2013; Wang et al., 2014) nor by AERONET aerosol retrievals (Li et al., 2014e) and as such appears less likely than an actual decrease in the global aerosol amount. For this reason we believe that the absence of any short-term AOT tendencies after 2002, confirmed by our new results, is more consistent with the actual preceding decrease in the tropospheric aerosol amount.

## 6. Conclusions

We have already mentioned that the length and the coverage of two major volcanic eruptions make the GACP aerosol record unique. One of the important previous findings based on the GACP record is a negative AOT trend between late 1980s and early 2000s. However, the AVHRR instruments on multiple NOAA satellites that were used to construct the combined GACP record were not designed for aerosol retrievals and have inherent limitations. Therefore, continued efforts are required to validate the GACP-based results and to establish whether they are consistent with other evidence.

This study provided several new lines of evidence, summarized below, that confirm the robustness of the GACP record and the previously identified negative AOT trend, as well as enhance our confidence in the interpretation of this trend.

The use of the NOAA-17 and NOAA-18 AVHRR data has allowed us to achieve three important objectives, as follows. First, the MODIS-based calibration of the NOAA-17 radiances in combination with the three-year overlap with the NOAA-16 and NOAA-17 aerosol retrievals confirmed the stability and robustness of the vicarious radiance calibration used to generate the previous GACP record. Second, the four-year

overlap between the NOAA-17 and NOAA-18 data allowed us to extend the GACP record by four years, through December 2009, and make it 26.5 years long. The simultaneous use of the NOAA-17 morning data and the NOAA-16 and -18 afternoon data has revealed high statistical correlation and considerably improved the spatial sampling density after August 2002. Third, we confirmed the negative nearly linear AOT trend that took place between the late 1980s and the early 2000s.

The PCA of the extended GACP record shows that most of the volcanic aerosol variability can be isolated into one mode responsible for  $\sim 12\%$  of the total variance. This conclusion is confirmed by the combined PCA analysis of the MODIS, MISR, and AVHRR GACP data during the volcano-free period from February 2000 to December 2009, which showed that the modes responsible for tropospheric-aerosol variability in the three datasets agree well in terms of correlation and spatial patterns.

The magnitude and duration of the negative AOT trend between the late 1980s and the early 2000s indicate that it was likely caused by a decrease in the tropospheric aerosol load. This conclusion was previously derived by Mishchenko et al. (2007a) and Mishchenko and Geogdzhayev (2007) and is consistent with the contemporaneous global brightening (Cermak et al., 2010; Wild, 2012, 2014). The decreasing AOT trend apparently ended by the early 2000s and was replaced by flat (on average) AOT values, which is in line with the MODIS and MISR AOT results as well as with the gradual transition from brightening to dimming observed recently in many aerosol producing regions (Wild, 2012, 2014). This finding, combined with recent black-carbon trend analyses, makes the attribution of the negative AOT trend to a contemporaneous global increase in aerosol absorption less plausible since the requisite global changes in aerosol composition appear to have been unlikely. We therefore interpret the flatness of the latest addition to the GACP record as a strong further evidence that the previously identified negative AOT trend is not artificial and is mostly due to a decrease in the tropospheric aerosol amount.

Our future plans include further validation of the updated GACP record using AERONET data as well as a further extension of the GACP record intended to make it current. These tasks will include a detailed analysis of the satellite-to-satellite transitions and will be greatly facilitated by the planned switch to a higher-sampling-density ISCCP product presently being developed.

## Acknowledgments

We thank two anonymous reviewers for insightful comments that have resulted in a much improved manuscript. This research was supported by the NASA Radiation Sciences Program managed by Hal Maring.

## Appendix A. Statistical analysis method

In this section we give a brief description of the method as applied to the previously described datasets. We begin by assuming that  $X$  is an  $N \times M$  data matrix, where  $N$  is the number of locations and  $M$  is the number of observations at each location. Prior to the analysis, each row of  $X$  is centered by removing the mean. Then the EOFs are found by determining the eigenvectors of the covariance matrix  $C$ , given by

$$C = XX^T / (M-1), \quad (4)$$

where  $T$  stands for “transposed”.  $C$  is an  $N \times N$  real positive semi-definite matrix, and can therefore be written as

$$C = E\Lambda E^T, \quad (5)$$

where  $\Lambda$  is a diagonal matrix whose elements are the  $N$  eigenvalues of  $C$  and  $E$  is an orthogonal matrix whose columns are the  $N$  orthogonal

eigenvectors, i.e., EOFs. Each EOF has a corresponding time series, the so-called principal components (PCs), and can be computed from

$$P = X^T E, \quad (6)$$

where  $P$  is a  $M \times N$  matrix whose columns are the  $N$  PCs. So  $P$  and  $E$  satisfy

$$X = EP^T. \quad (7)$$

Combining Eqs. (4), (5), and (7), we can see that

$$\Lambda = P^T P / (M-1). \quad (8)$$

Since  $\Lambda$  is diagonal, the PCs are mutually orthogonal and the eigenvalues are equal to their variances.

The (CPCA) is used to assess the AVHRR tropospheric aerosol modes using Terra-MODIS and MISR data. Mathematically, the CPCA finds the modes that maximize the variance explained by the sum of the elements in the combined fields (Bretherton et al., 1992). Let the three  $N \times M$  AOT data fields from each instrument be  $X$ ,  $Y$ , and  $Z$ , where  $N$  is the number of locations and  $M$  is the number of observations. Before the analysis, each row of  $X$ ,  $Y$ , and  $Z$  is again centered by removing the mean. The combined  $3N \times M$  data matrix is constructed as according to

$$D = \begin{bmatrix} X \\ Y \\ Z \end{bmatrix}. \quad (9)$$

The temporal covariance matrix is

$$C = \frac{1}{M-1} D D^T. \quad (10)$$

The spatial patterns, or (EOFs), are found by determining the eigenvectors of  $C$ :

$$C = E \Lambda E^T, \quad (11)$$

where  $E$  is a  $3N \times 3N$  orthogonal matrix.  $\Lambda$  is a diagonal matrix whose elements are the eigenvalues of  $C$ , sorted in descending order. The first  $N$  elements of each column of  $E$  form the EOFs of  $X$ , the next  $N$  elements form the EOFs of  $Y$ , and the last  $N$  elements are the EOFs of  $Z$ . The expansion coefficients of each EOF mode, or (PCs), are determined by projecting the data matrix onto each EOF according to

$$\vec{P}_i = D^T \vec{E}_i. \quad (12)$$

It can be shown that the PCs are also orthogonal and the elements of the diagonal matrix  $\Lambda$  are their variances. Let  $\lambda_i$  be the  $i$ th element of  $\Lambda$ ; then the fraction of variance ( $FV$ ) explained by the  $i$ th mode is

$$FV = \lambda_i / \sum \lambda_i. \quad (13)$$

More examples of CPCA analyses of aerosol observational datasets can be found in Li et al. (2014c).

## References

Bjornsson, H., Venegas, S.A., 1997. A manual for EOF and SVD analysis of climate data. CCGCR Rep. 97-1. McGill University, Montréal, QC, Canada.

Bond, T.C., Doherty, S.J., Fahey, D.W., et al., 2013. Bounding the role of black carbon in the climate system: a scientific assessment. *J. Geophys. Res. Atmos.* 118, 5380–5552.

Brest, C.L., Rossow, W.B., Roiter, M.D., 1997. Update of radiance calibration for ISCCP. *J. Atmos. Ocean. Technol.* 14, 1091–1109.

Bretherton, C.S., Smith, C., Wallace, J.M., 1992. An intercomparison of methods for finding coupled patterns in climate data. *J. Clim.* 5, 541–560.

Cermak, J., Wild, M., Knutti, R., Mishchenko, M.I., Heidinger, A.K., 2010. Consistency of global satellite-derived aerosol and cloud data sets with recent brightening observations. *Geophys. Res. Lett.* 37, L21704.

Che, N., Price, J.C., 1992. Survey of radiometric calibration results and methods for visible and near infrared channels of NOAA-7, -9, and -11 AVHRRs. *Remote Sens. Environ.* 41, 19–27.

Chin, M., Diehl, T., Tan, Q., Prospero, J.M., Kahn, R.A., Remer, L.A., et al., 2014. Multi-decadal aerosol variations from 1980 to 2009: a perspective from observations and a global model. *Atmos. Chem. Phys.* 14, 3657–3690.

Diner, D., Beckert, J., Reilly, T., Bruegge, C.J., Conel, J.E., Kahn, R.A., et al., 1998. Multiangle Imaging Spectroradiometer (MISR) description and experiment overview. *IEEE Trans. Geosci. Remote Sens.* 36, 1072–1087.

Geogdzhayev, I.V., Mishchenko, M.I., Rossow, W.B., Cairns, B., Laci, A.A., 2002. Global two-channel AVHRR retrievals of aerosol properties over the ocean for the period of NOAA-9 observations and preliminary retrievals using NOAA-7 and NOAA-11 data. *J. Atmos. Sci.* 59, 262–278.

Geogdzhayev, I.V., Mishchenko, M.I., Terez, E.I., Terez, G.A., Gushchin, G.K., 2005. Regional advanced very high resolution radiometer-derived climatology of aerosol optical thickness and size. *J. Geophys. Res.* 110, D23205.

Geogdzhayev, I.V., Cairns, B., Mishchenko, M.I., Tsigaridis, K., van Noije, T., 2014. Model-based estimation of sampling-caused uncertainty in aerosol remote sensing for climate research applications. *Q. J. R. Meteorol. Soc.* 140, 2353–2363.

Hansen, J.E., Travis, L.D., 1974. Light scattering in planetary atmospheres. *Space Sci. Rev.* 16, 27–610.

Hansen, J., Nazarenko, L., Ruedy, R., Sato, M., Willis, J., Del Genio, A., et al., 2005. Earth's energy imbalance: confirmation and implications. *Science* 308, 1431–1435.

Heidinger, A.K., Straka III, W.C., Molling, C.C., Sullivan, J.T., Wu, X., 2010. Deriving an inter-sensor consistent calibration for the AVHRR solar reflectance data record. *Int. J. Remote Sens.* 31, 6493–6517.

IPCC, 2007. Summary for policymakers. In: Solomon, S., Qin, D., Manning, M., Chen, Z., Marquis, M., Averyt, K.B., Tignor, M., Miller, H.L. (Eds.), *Climate Change: The Physical Science Basis*. Cambridge University Press, Cambridge, UK.

Kahn, R., Nelson, D., Garay, M., Levy, R., Bull, M., Diner, D., et al., 2009. MISR aerosol product attributes and statistical comparisons with MODIS. *IEEE Trans. Geosci. Remote Sens.* 47, 4095–4114.

Kaufman, Y.J., Holben, B.N., 1993. Calibration of the AVHRR visible and near-IR bands by atmospheric scattering, ocean glint and desert reflection. *Int. J. Remote Sens.* 14, 21–52.

Kiehl, J.T., 2007. Twentieth century climate model response and climate sensitivity. *Geophys. Res. Lett.* 34, L22710.

King, M.D., Menzel, W.P., Kaufman, Y.J., Tanré, D., Gao, B.C., Platnick, S., et al., 2003. Cloud and aerosol properties, precipitable water, and profiles of temperature and water vapor from MODIS. *IEEE Trans. Geosci. Remote Sens.* 41, 442–458.

Laci, A.A., Oinas, V., 1991. A description of the correlated k-distribution method for modeling non-grey gaseous absorption, thermal emission, and multiple scattering in vertically inhomogeneous atmospheres. *J. Geophys. Res.* 96, 9027–9063.

Levy, R.C., 2009. The dark-land MODIS collection 5 aerosol retrieval: algorithm development and product evaluation. In: Kokhanovsky, A.A., de Leeuw, G. (Eds.), *Satellite Aerosol Remote Sensing Over Land*. Praxis, Chichester, UK, pp. 19–68.

Levy, R.C., Remer, L.A., Kleidman, R.G., Mattoo, S., Ichoku, C., Kahn, R., Eck, T.F., 2010. Global evaluation of the Collection 5 MODIS dark-target aerosol products over land. *Atmos. Chem. Phys.* 10, 10399–10420.

Li, J., Carlson, B.E., Laci, A.A., 2013. Application of spectral analysis techniques in the inter-comparison of aerosol data, part I: an EOF approach to analyze the spatial-temporal variability of aerosol optical depth using multiple remote sensing data sets. *J. Geophys. Res. Atmos.* 118, 8640–8648.

Li, J., Carlson, B.E., Laci, A.A., 2014a. Revisiting AVHRR tropospheric aerosol trends using principal component analysis. *J. Geophys. Res. Atmos.* 119, 3309–3320.

Li, J., Carlson, B.E., Laci, A.A., 2014b. Application of spectral analysis techniques in the inter-comparison of aerosol data. Part II: using maximum covariance analysis to effectively compare spatio-temporal variability of satellite and AERONET measured aerosol optical depth. *J. Geophys. Res.* 119, 153–166.

Li, J., Carlson, B.E., Laci, A.A., 2014c. Application of spectral analysis techniques in the inter-comparison of aerosol data. Part III: using combined PCA to compare spatio-temporal variability of MODIS, MISR and OMI aerosol optical depth. *J. Geophys. Res. Atmos.* 119, 4017–4042.

Li, C., Xue, Y., Liu, Q., Guang, J., He, X., Zhang, J., et al., 2014d. Post calibration of channels 1 and 2 of long-term AVHRR data record based on SeaWiFS data and pseudo-invariant targets. *Remote Sens. Environ.* 150, 104–119.

Li, J., Carlson, B.E., Dubovik, O., Laci, A.A., 2014e. Recent trends in aerosol optical properties derived from AERONET measurements. *Atmos. Chem. Phys.* 14, 12271–12289.

Liu, L., Mishchenko, M.I., Geogdzhayev, I.V., Smirnov, A., Sakerin, S.M., Kabanov, D.M., Ershov, O.A., 2004. Global validation of two-channel AVHRR aerosol optical thickness retrievals over the oceans. *J. Quant. Spectrosc. Radiat. Transf.* 88, 97–109.

Loeb, N.G., Su, W., 2010. Direct aerosol radiative forcing uncertainty based on a radiative perturbation analysis. *J. Clim.* 23, 5288–5293.

Lohmann, U., Ferrachat, S., 2010. Impact of parametric uncertainties on the present-day climate and on the anthropogenic aerosol effect. *Atmos. Chem. Phys.* 10, 11373–11383.

Martonchik, J.V., Kahn, R.A., Diner, D.J., 2009. Retrieval of aerosol properties over land using MISR observations. In: Kokhanovsky, A.A., de Leeuw, G. (Eds.), *Satellite Aerosol Remote Sensing Over Land*. Praxis, Chichester, UK, pp. 267–293.

McClatchey, R.A., Fenn, R.W., Selby, J.E.A., Volz, F.E., Garing, J.S., 1972. Optical properties of the atmosphere. Environmental Research Paper 411. Air Force Cambridge Research Laboratory, Bedford, MA.

Mishchenko, M.I., Geogdzhayev, I.V., 2007. Satellite remote sensing reveals regional tropospheric aerosol trends. *Opt. Express* 15, 7423–7438.

Mishchenko, M.I., Travis, L.D., 1997. Satellite retrieval of aerosol properties over the ocean using polarization as well as intensity of reflected sunlight. *J. Geophys. Res.* 102, 16989–17013.

- Mishchenko, M.I., Geogdzhayev, I.V., Cairns, B., Rossow, W.B., Laci, A.A., 1999. Aerosol retrievals over the ocean using channel 1 and 2 AVHRR data: a sensitivity analysis and preliminary results. *Appl. Opt.* 38, 7325–7341.
- Mishchenko, M., Penner, J., Anderson, D., editors, 2002a. *Global Aerosol Climatology Project*. *J. Atmos. Sci.* 59, 249–783.
- Mishchenko, M.I., Travis, L.D., Laci, A.A., 2002b. *Scattering, Absorption, and Emission of Light by Small Particles*. Cambridge University Press, Cambridge, UK.
- Mishchenko, M.I., Geogdzhayev, I.V., Liu, L., Ogren, J.A., Laci, A.A., Rossow, W.B., et al., 2003. Aerosol retrievals from AVHRR radiances: effects of particle nonsphericity and absorption and an updated long-term global climatology of aerosol properties. *J. Quant. Spectrosc. Radiat. Transf.* 79–80, 953–972.
- Mishchenko, M.I., Geogdzhayev, I.V., Rossow, W.B., Cairns, B., Carlson, B.E., Laci, A.A., et al., 2007a. Long-term satellite record reveals likely recent aerosol trend. *Science* 315, 1543.
- Mishchenko, M.I., Geogdzhayev, I.V., Cairns, B., Carlson, B.E., Chowdhary, J., Laci, A.A., et al., 2007b. Past, present, and future of global aerosol climatologies derived from satellite observations: a perspective. *J. Quant. Spectrosc. Radiat. Transf.* 106, 325–347.
- Mishchenko, M.I., Geogdzhayev, I.V., Liu, L., Laci, A.A., Cairns, B., Travis, L.D., 2009. Toward unified satellite climatology of aerosol properties: what do fully compatible MODIS and MISR aerosol pixels tell us? *J. Quant. Spectrosc. Radiat. Transf.* 110, 402–408.
- Mishchenko, M.I., Liu, L., Geogdzhayev, I.V., Li, J., Carlson, B.E., Laci, A.A., Cairns, B., Travis, L.D., 2012. Aerosol retrievals from channel-1 and -2 AVHRR radiances: long-term trends updated and revisited. *J. Quant. Spectrosc. Radiat. Transf.* 113, 1974–1980.
- Penner, J.E., Xu, L., Wang, M., 2011. Satellite methods underestimate indirect climate forcing by aerosols. *Proc. Natl. Acad. Sci. U. S. A.* 108, 13404–13408.
- Rao, C.R.N., Chen, J., 1995. Inter-satellite calibration linkages for the visible and near-infrared channels of the AVHRR on the NOAA-7, -9 and -11 spacecraft. *Int. J. Remote Sens.* 16, 1931–1942.
- Remer, L., Kleidman, R.G., Levy, R.C., Kaufman, Y.J., Tanré, D., Mattoo, S., et al., 2008. Global aerosol climatology from the MODIS satellite sensors. *J. Geophys. Res.* 113, D14S07.
- Rossow, W., Ferrier, J., 2015. Evaluation of long-term calibrations of the AVHRR visible radiances. *J. Atmos. Ocean. Technol.* 32, 744–766.
- Rossow, W.B., Garder, L.C., 1993a. Cloud detection using satellite measurements of infrared and visible radiances for ISCCP. *J. Clim.* 6, 2341–2369.
- Rossow, W.B., Garder, L.C., 1993b. Validation of ISCCP cloud detection. *J. Clim.* 6, 2370–2393.
- Rossow, W.B., Schiffer, R.A., 1999. Advances in understanding clouds from ISCCP. *Bull. Am. Meteorol. Soc.* 80, 2261–2287.
- Smirnov, A., Holben, B.N., Sakerin, S.M., Kabanov, D.M., Slutsker, I., Chin, M., et al., 2006. Ship-based aerosol optical depth measurements in the Atlantic Ocean: comparison with satellite retrievals and GOCART model. *Geophys. Res. Lett.* 33 L14817.
- Tanré, D., Bréon, F.M., Deuzé, J.L., Dubovik, O., Ducos, F., François, P., et al., 2011. Remote sensing of aerosols by using polarized, directional and spectral measurements within the A-Train: the PARASOL mission. *Atmos. Meas. Tech.* 4, 1383–1395.
- Wang, R., Tao, S., Shen, H., Huang, Y., Chen, H., Balkanski, Y., Boucher, O., Ciais, P., Shen, G., Li, W., Zhang, Y., Chen, Y., Lin, N., Su, S., Li, B., Liu, J., Liu, W., 2014. Trend in global black carbon emissions from 1960 to 2007. *Environ. Sci. Technol.* 48, 6780–6787.
- Wild, M., 2012. Enlightening global dimming and brightening. *Bull. Am. Meteorol. Soc.* 93, 27–37.
- Wild, M., 2014. Global dimming and brightening. In: Freedman, B. (Ed.), *Global Environmental Change*. Springer, Berlin, pp. 39–47.
- Yoon, J., Burrows, J.P., Vountas, M., von Hoyningen-Huene, W., Chang, D.Y., Richter, A., Hilboll, A., 2014. Changes in atmospheric aerosol loading retrieved from space-based measurements during the past decade. *Atmos. Chem. Phys.* 14, 6881–6902.
- Zerefos, C.S., Tourpali, K., Eleftheratos, K., Kazadzis, S., Meleti, C., Feister, U., et al., 2012. Evidence of a possible turning point in solar UV-B over Canada, Europe and Japan. *Atmos. Chem. Phys.* 12, 2469–2477.
- Zhang, J., Reid, J.S., 2010. A decadal regional and global trend analysis of the aerosol optical depth using a data-assimilation grade over-water MODIS and Level 2 MISR aerosol products. *Atmos. Chem. Phys.* 10, 10949–10963.
- Zhao, T.X.-P., Laszlo, I., Guo, W., Heidinger, A., Cao, C., Jelenak, A., et al., 2008. Study of long-term trend in aerosol optical thickness observed from operational AVHRR satellite instrument. *J. Geophys. Res.* 113, D07201.